# Antiviral Drugs from the Nucleoside Analog Family Block Volume-Activated Chloride Channels

Martin Gschwentner,* Alex Susanna,* Ewald Wöll,†
Markus Ritter,† Ulrich O. Nagl,* Andreas Schmarda,*
Andreas Laich,* Germar M. Pinggera,* Helmut Ellemunter,‡
Hartwig Huemer,§ Peter Deetjen,* and Markus Paulmichl*

*Department of Physiology, †Department of Internal Medicine,
‡Department of Pediatrics, and §Department of Hygiene, University of
Innsbruck, Innsbruck, Austria

## ABSTRACT

**Background:** The antiviral drugs AZT and acyclovir are generally used in the treatment of infections with human immunodeficiency virus (HIV) and herpes simplex virus (HSV). These substances are known to impede virus replication by premature nucleic acid chain termination. It is not yet clear, however, if this is the sole mechanism responsible for the antiviral and/or the numerous side effects observed in patients treated with these agents. We investigated the swelling-induced chloride current in fibroblasts, which we demonstrated is closely related or identical to a cloned epithelial chloride channel, $I_{Cln}$. This chloride channel can be blocked by nucleotides.

**Materials and Methods:** Electrophysiological, fluorescence optical, and volume measurements were made to determine the effect of nucleoside analogs on the swell-ing-dependent chloride current ($I_{Cl}$) in NIH 3T3 fibroblasts and in human T cell lymphoma (H9) cells and the cAMP-dependent chloride current in CaCo cells.

**Results:** AZT and acyclovir block the swelling-dependent chloride current and the chloride flux in fibroblasts, and the regulatory volume decrease (RVD) and $I_{Cl}$ in H9 cells. This immediate effect can be substantially reduced by the simultaneous incubation of the cells with thymidine-5'-diphosphate (TDP) or uridine, both of which are by themselves unable to affect $I_{Cl}$.

**Conclusions:** We show here a novel molecular mechanism by which antiviral drugs of the nucleoside analog family could lead to impairments of the kidney, bone marrow, gastrointestinal, and neuronal functions, and how these side effects could possibly be restricted by the presence of TDP or uridine.

## INTRODUCTION

The use of nucleoside analogs is a major strategy in the treatment of viral infections. The key mechanism by which these substances interfere with virus replication appears to be by inducing premature chain termination; it is still unclear, however, if this is the exclusive antiviral effect and how different side effects observed both in vitro and in patients treated with these drugs can be explained. The side effects consist mainly of bone marrow suppression and impaired central and peripheral neuronal tissue, gastrointestinal tissue, and kidney function. This organ preference for the side effects of these drugs seems to result from mechanisms different from premature chain termination. As previously demonstrated, $I_{Cln}$, a chloride channel cloned from epithelial cells and expressed in *Xenopus laevis* oocytes, can be blocked by the addition of different nucleotides (cGMP, ITP, cAMP, GTP, ATP, ADP, or AMP) to the extracellular solution (1). A similar nucleotide block of chloride currents has recently been shown in other cell systems (2–4). Mutation of a putative nucleotide binding region in $I_{Cln}$ leads to a dramatic reduction of the nu-

Correspondence address and reprint requests to: Markus Paulmichl, Department of Physiology, University of Innsbruck, Fritz-Pregl-Strasse 3, A-6020 Innsbruck, Austria.

cleotide block and to a change in the kinetics of the current expressed in oocytes (1). In NIH 3T3 fibroblasts, the swelling-induced chloride current ($I_{Cl}$) can similarly be blocked by cAMP, cGMP, or ATP. This endogenous current can be significantly reduced by antisense oligonucleotides against $I_{Cln}$, indicating that $I_{Cln}$ is the prevalent protein involved in $I_{Cl}$ (5). The aim of the present study was to investigate the effect of antiviral drugs from the nucleoside analog family on $I_{Cl}$. We show here that nucleoside analogs selectively block $I_{Cl}$ and the regulatory volume decrease (RVD) at concentrations one to two orders of magnitude lower than nucleotides, thus interfering with a vital cell regulatory mechanism at concentrations present in the plasma of patients treated with these drugs.

## MATERIAL AND METHODS

### Electrophysiology and Cell Culture

The whole-cell voltage clamp method (6) was chosen to measure swelling-induced chloride currents in isolated NIH 3T3 fibroblasts, colon carcinoma (CaCo) cells, and H9 cells, a human T cell lymphoma cell line (ATCC HTB 176). Fibroblasts and CaCo cells were grown on glass cover slips in Dulbecco's modified Eagle's medium (DMEM) supplemented with 10% fetal calf serum, 4 mM glutamine, 100 IU/ml penicillin, 100 μg/ml streptomycin at 37°C, 5% $CO_2$, 95% air, and measured 24–48 hr after splitting. H9 cells were grown in suspension in RPMI-1640 medium supplemented with 10% fetal calf serum, 2 mM glutamine, 100 IU/ml penicillin, 100 μg/ml streptomycin at 37°C, 5% $CO_2$, 95% air. For electrical measurements in H9 cells, glass cover slips were coated with a 0.25% collagen solution (type I). All experiments were carried out at room temperature (20–22°C). Bath and pipette solutions were chosen to enable chloride current measurements. The isotonic extracellular solution used was composed of (in mM): NaCl 125, $CaCl_2$ 2.5, $MgCl_2$ 2.5, N-2-hydroxyethylpipera-zine-N'-2-ethanesulfonic acid (HEPES) 10, mannitol 50, pH 7.2 (adjusted with NaOH). Mannitol was omitted to reduce extracellular osmolarity. One to two minutes after confirming whole-cell configuration, hypotonic conditions were established and the activated outwardly rectifying chloride current measured. Fast exchange of the bath solution was obtained using a perfusion system with a flow rate of 10 ml/min and a bath

volume of ≈250 μl. The blocking effect on $I_{Cl}$ of the different substances tested was determined 2–4 min after the addition of the corresponding concentrations to the extracellular solution. The filling solution of the patch pipette was (in mM): CsCl 144, $MgCl_2$ 5, ethyleneglycol-bis(β-amino-ethyl ether)-N,N,N',N'-tetraacetic acid (EGTA) 11, HEPES 10, pH 7.2 (adjusted with CsOH). For data acquisition and analysis an EPC-9 (HEKA, Lambrecht, Germany) and an Axopatch 200A (Axon Instruments, Foster City, CA U.S.A.) amplifier, controlled by an Atari or an Apple computer running the according software for driving the amplifier and PULSE and REVIEW for analysis (Instrutech, Great Neck, NY U.S.A.) was used. All current measurements were filtered at 1 kHz (analog 4-pole BESSEL) and leak subtracted where indicated. Where applicable, data are expressed as arithmetic means ± standard error of the mean (SEM). Statistical analysis was made by $t$-test where appropriate. Significant difference was assumed at $p < 0.05$.

### Fluorescence Optical Measurements

CHLORIDE MEASUREMENTS USING MEQ. NIH 3T3 fibroblasts were superfused with a hypotonic solution containing (in mM): Na-gluconate 81, K gluconate 5.4, $MgSO_4$ 0.8, Ca-gluconate 1.2, $NaH_2PO_4$ 1, glucose 5.5, Tris(hydroxymethyl) aminomethane (Tris) 5, pH adjusted to 7.4. At the point indicated (arrow in Fig. 1d), the hypotonic extracellular fluid was changed to a solution containing 150 mM KSCN. The decrease of fluorescence is proportional to chloride permeability ($P_{Cl}$) since $SCN^-$ is able to quench MEQ (6-methoxy-N-ethylquinolinium iodide) fluorescence more effectively than chloride (7), $I_{Cln}$ is more permeable for $SCN^-$ than for chloride (8), and $I_{Cl}$ is reduced by only ≈40% within the first 180 sec after restoring normal osmolarity. Fluorescence measurements were made under an inverted microscope equipped for epifluorescence and photometry. Light from a xenon arc lamp was directed through a grey filter (nominal transmission 0.3%) and a 340 ± 10 nm interference filter, deflected by a dichroic mirror and directed through the objective. The emitted light was directed through a 420 nm cutoff filter to a cooled photomultiplier tube for photon counting (9). For loading the cells with MEQ it is essential to convert MEQ to diH-MEQ (6-methoxy-N-ethyl 1,2-dihydroquinolinium iodide; methods are described in Ref. 10). The fibroblasts were

incubated for 10 minutes in a 5-$\mu$M diH-MEQ solution (37°C, 5% $CO_2$), washed with PBS and incubated in DMEM for another 10 min prior to measurement.

*VIABILITY MEASUREMENTS.* Viability of NIH 3T3 fibroblasts was measured using a confocal microscope (LSM 410, Zeiss, Oberkochen, Germany) after labeling the cells with calcein AM and ethidium homodimer (11). Cells were grown on sterile glass cover slips (see above) and incubated for 20 min with 2 $\mu$M calcein AM and 4 $\mu$M ethidium homodimer as described by the supplier (EucoLight, Molecular Probes, Eugene, OR, U.S.A.). After washing the cells with PBS the cover slips were mounted under an inverted laser scan microscope (LSM 410). The fluorescent dyes were excited by an argon laser (488 nm). Fluorescence emission from both fluorophores was viewed simultaneously using a dichroic mirror (FT580) and two emission filters (530 nm bandpass for calcein and 590 nm longpass for ethidium homodimer, respectively). Live cells were distinguished by the presence of intracellular esterase activity, determined by enzymatic conversion of nonfluorescent calcein AM to green fluorescent calcein, whereas dead cells with damaged membranes were entered by ethidium homodimer, leading to red fluorescence after binding to nucleic acids. Viable cells are expressed as percentage of total cell number in a given area.

## Cell Volume Measurements

Cell volume was measured in 30-sec intervals using a Casy-1 model TT (Schärfe, Reutlingen, Germany). The measurements were made after splitting the cells and growing the single cells for 12, 24, and 34 hr in the incubator. Cell volume was calculated from the median of the cell volume distribution curves using latex beads as calibration standards (12,13). During measurement cells were kept at 30–37°C. The isotonic extracellular solution for volume measurements was (in mM): NaCl 90, mannitol 80, KCl 5.4, $MgCl_2$ 0.8, $CaCl_2$ 1.2, glucose 5.5, tris(hydroxymethyl) aminomethane (Tris) 5, pH 7.4 (adjusted with NaOH). To reduce extracellular osmolarity the isotonic solution was diluted with a solution composed as above but missing mannitol. Final osmolality of the different solutions was verified by freezing point depression.

# RESULTS

## The Swelling-Induced Chloride Current Can Be Blocked by Nucleoside Analogs Such as AZT or Acyclovir

A chloride current of $+97.7 \pm 11$ pA ($+40$ mV; $n = 44$) can be measured in NIH 3T3 fibroblasts (passages 60–100) under isotonic conditions. Reducing extracellular osmolarity (omitting 50 mM mannitol) leads to a marked increase in the current to $+1473.6 \pm 104$ pA ($n = 44$). As shown in Fig. 1, the thymidine nucleoside analog 3'-azido-3'-deoxythymidine (AZT) blocks the swelling-induced chloride current ($I_{Cl}$) at a half maximal concentration ($IC_{50}$) of $\approx 20$ $\mu$M (Fig. 1 a and b), with the block being equally effective on both current directions (Fig. 1c) 3–4 min after adding the drug to the extracellular solution.

In addition to the electrophysiological measurements, the effect of AZT on chloride transport is also demonstrated using a fluorescence optical technique. As depicted in Fig. 1d, cells challenged with a hypotonic solution show substantial chloride permeability ($P_{Cl}$) across the cell membrane (see Materials and Methods). In the presence of AZT, $P_{Cl}$ is significantly reduced.

The antiviral drug acyclovir blocks $I_{Cl}$ similarly to AZT ($IC_{50} \approx 10$ $\mu$M; Fig. 2a). In contrast, ganciclovir, a compound comprised of acyclovir and an additional hydroxymethyl group at the "sugar rudiment", has no significant effect on $I_{Cl}$ up to a concentration of 0.1 mM (Fig. 2b).

## The Nucleoside Block Can Be Influenced by the Addition of TDP and Uridine

In contrast to AZT, the nucleotide thymidine-5'-diphosphate (TDP) is not able to block $I_{Cl}$ at concentrations up to 0.1 mM (Fig. 3a). In the presence of 0.1 mM TDP, the addition of 0.1 mM AZT has only a minute blocking effect (Fig. 3b). After washing out TDP and AZT, however, the renewed addition of 0.1 mM AZT alone dramatically reduces $I_{Cl}$ (Fig. 3b). Similar effects were obtained using uridine in combination with acyclovir. In the presence of 100 $\mu$M uridine, the chloride current elicited by reducing extracellular osmolarity ($I_{Cl}$) is $+1321.0 \pm 191.4$ pA ($+40$ mV; $n = 8$). Adding 100 $\mu$M acyclovir does not significantly change the current ($+1223.2 \pm 252.3$ pA; $n = 8$). However, omitting both uridine and acyclovir, and adding 100 $\mu$M acyclovir alone leads to a substantial reduction of $I_{Cl}$ to $+493.9 \pm 100.7$ pA ($n = 8$) in the same cells. Uridine, as well as TDP, prevents nucleoside an-
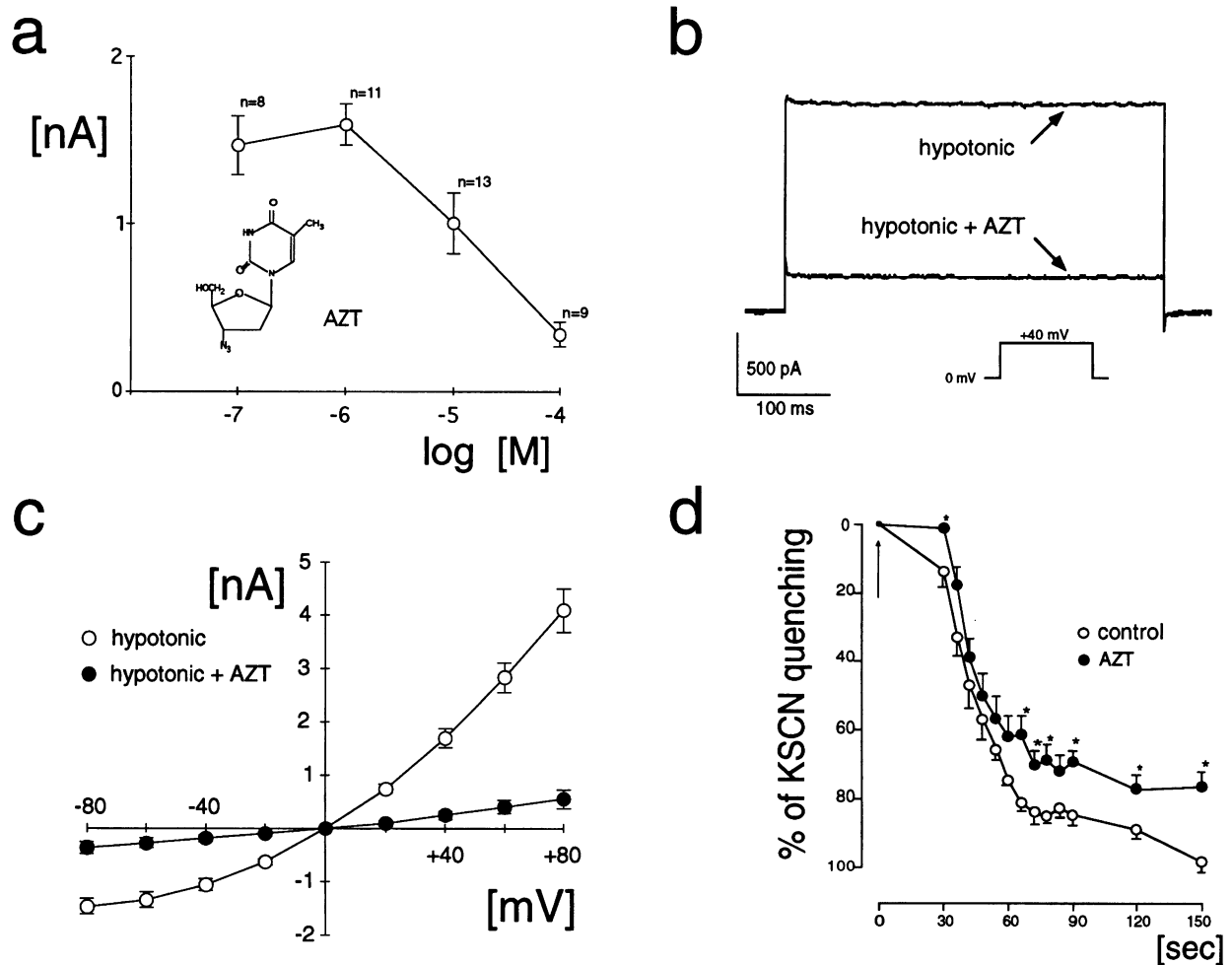
**FIG. 1.    Inhibition of the swelling-induced chloride current ($I_{Cl}$) and chloride permeability by the antiviral drug azidothymidine (3′-azido-3′-deoxythymidine, AZT) in NIH 3T3 fibroblasts**

(a) AZT blocks $I_{Cl}$ irreversibly. The cells were held at 0 mV and clamped repetitively to a potential of +40 mV for 400 msec (all values given without leak subtraction). Current measurements were taken 1–5 min after drug application. The insert depicts the molecular structure of the compound used. (b) Original tracing showing the inhibitory effect of 100 $\mu$M AZT (hypotonic + AZT) on the swelling-induced chloride current (hypotonic) in the same NIH 3T3 fibroblast. Voltage clamp protocol as above. (c) Current voltage relation of the swelling-induced chloride current in the absence (hypotonic; open symbols) and presence of 100 $\mu$M AZT (hypotonic + AZT; closed symbols). The cells were held at 0 mV and voltage steps made for 800 msec from −80 mV to +80 mV in 20 mV increments. The current measurements after decreasing extracellular osmolarity are −1466 ± 143 pA, −1053 ± 107 pA, +1692 ± 184 pA, and +4091 ± 404 pA in the absence of AZT, and −367 ± 111 pA, −185 ± 59 pA, +248 ± 76 pA, and +551 ± 170 pA in the presence of AZT at −80 mV, −40 mV, +40 mV, and +80 mV, respectively (for both, $n$ = 5; peak current was measured 10 msec after pulse onset). (d) Measurements of chloride permeability ($P_{Cl}$) in NIH 3T3 fibroblasts in the absence (control) and presence of 100 $\mu$M AZT (AZT). Independent measurements of eight cells in the absence and nine cells in the presence of AZT are summarized as total percentage of the KSCN-quenchable MEQ signal plotted for a time frame of 30–150 sec after addition of KSCN (% KSCN quenching; see Materials and Methods).
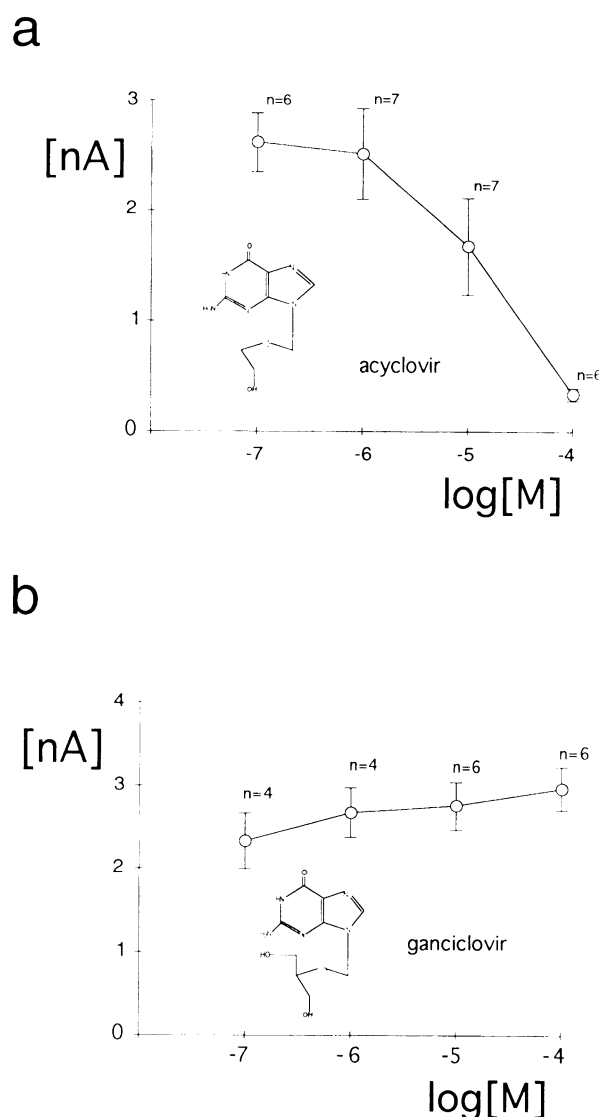
## a



## a



## b



## b



**FIG. 2.  Effect of acyclovir and ganciclovir on the swelling-induced chloride current in NIH 3T3 fibroblasts**

(a) Half maximal blocking effect of acyclovir is observed at a concentration of $\approx 10$ $\mu$M. (b) Ganciclovir is without significant effect on $I_{Cl}$ at concentrations up to 0.1 mM. The inserts depict the molecular structures of the compounds used.

**FIG. 3.  The effect of thymidine 5'-diphosphate on $I_{Cl}$ in NIH 3T3 fibroblasts**

(a) Thymidine 5'-diphosphate (TDP) added to the extracellular fluid is without significant effect on $I_{Cl}$ at concentrations up to 100 $\mu$M (the insert depicts the molecular structure of the compound used). (b) Addition of 100 $\mu$M AZT on top of 100 $\mu$M TDP only scarcely reduces $I_{Cl}$. However, after washing out the TDP-AZT mixture, addition of 100 $\mu$M AZT markedly reduces $I_{Cl}$ ($n = 6$).

alogs from blocking $I_{Cl}$, most likely by competitive binding.

## The Swelling-Induced Chloride Current in T Cell Lymphoma Cells Is Sensitive to AZT and Acyclovir

Swelling-induced chloride currents sensitive to nucleotides have been shown in epithelial cells (2–4), which could act as possible targets for viral
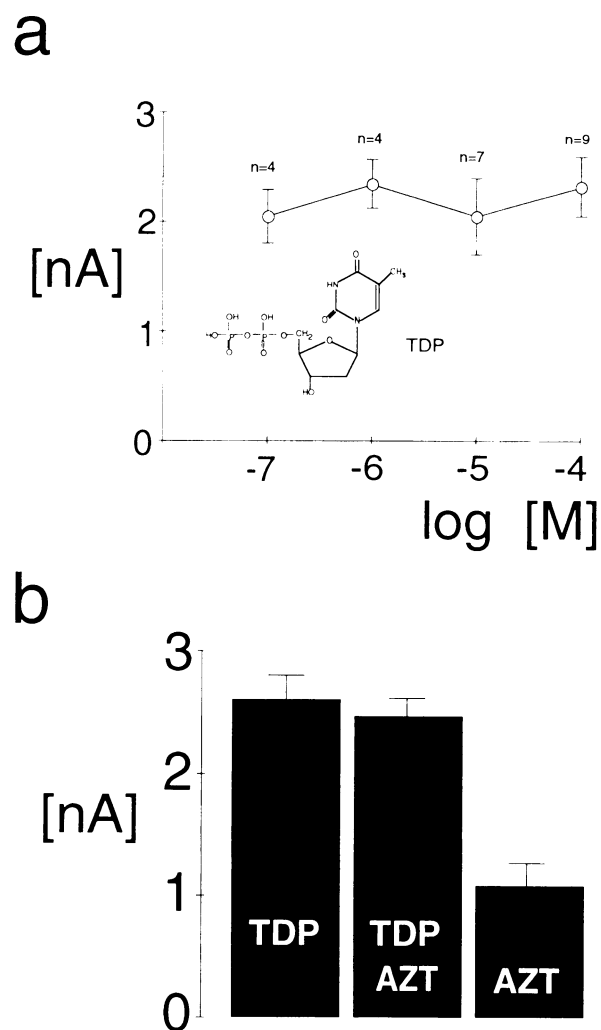
infections. Since AZT is an essential drug in the treatment of human immunodeficiency virus (HIV) and T cells are the major target of HIV, we investigated whether $I_{Cl}$ sensitivity to AZT can be measured in H9 cells, a human T cell lymphoma line. The $I_{Cl}$ induced in H9 cells is as sensitive to AZT or acyclovir as $I_{Cl}$ in NIH 3T3 fibroblasts ($IC_{50}$ for AZT $\approx 30$ $\mu$M and for acyclovir $\approx 20$ $\mu$M; Fig. 4 a and b). It has been shown that $I_{Cl}$, the swelling-induced chloride current is identical to $I_{Cln}$ or closely related to it (5). Blocking these
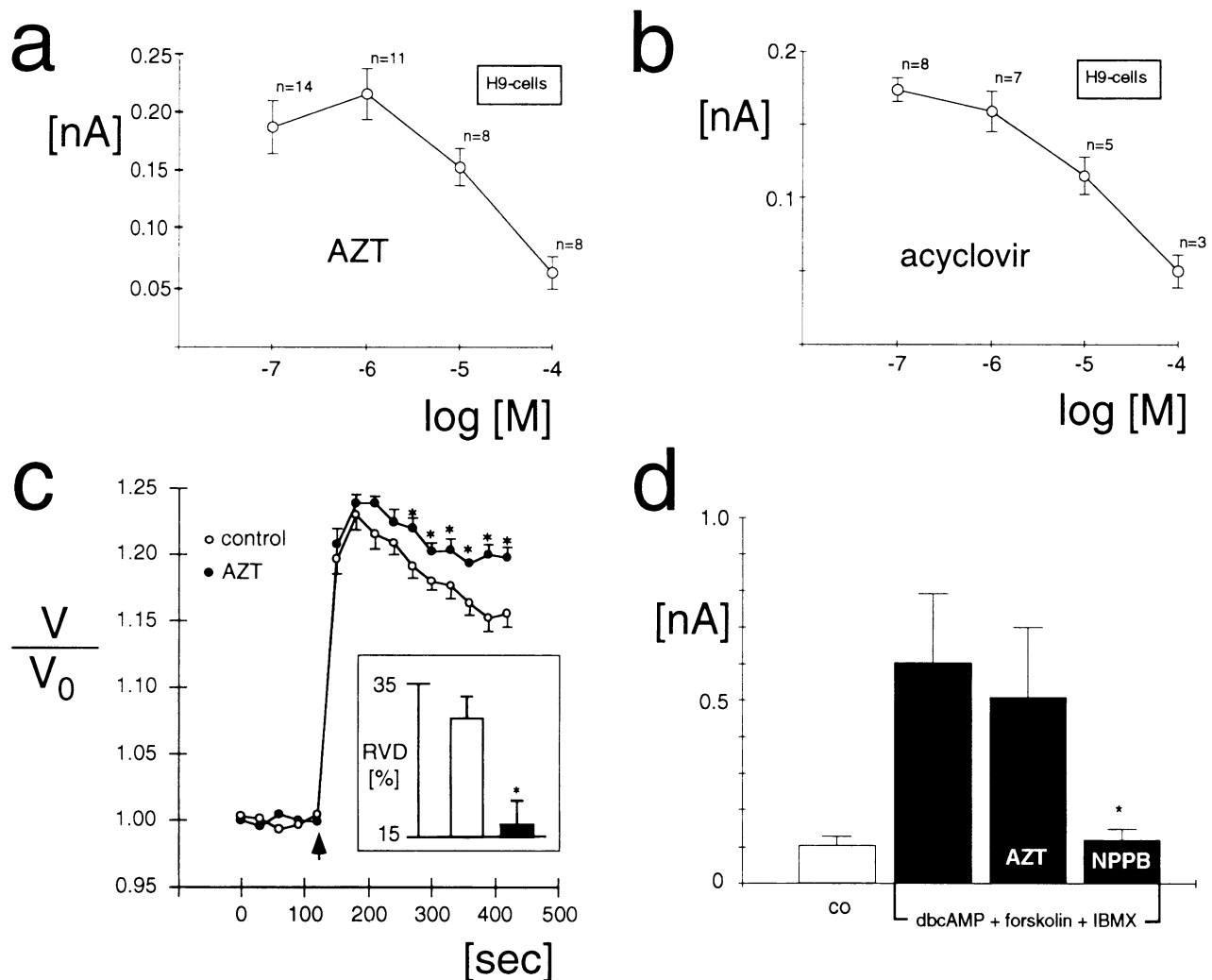
FIG. 4. AZT and acyclovir block the swelling-induced chloride current and regulatory volume decrease (RVD) in the human T cell lymphoma cell line H9

(a) In H9 cells (pulse protocol see Fig. 1a), half maximal blockage can be observed at a concentration of $\approx 30$ $\mu$M AZT added to the extracellular solution. Currents are leak subtracted. (b) Dose response curve for acyclovir added to the extracellular fluid ($IC_{50} \approx 20$ $\mu$M). Currents are leak subtracted. (c) AZT significantly impedes regulatory volume decrease (RVD) in H9 cells: following reduction of extracellular osmolarity by 70 mosM H9 cells display instant cell swelling to 123.0 ± 1.1% ($n = 8$) in the absence (open symbols) and to 123.9 ± 0.6% ($n = 9$) in the presence of AZT (closed symbols). Under control conditions this cell swelling is followed by a gradual reduction of cell volume to 116.0 ± 0.9% ($n = 6$) within 240 sec after peak volume. In the presence of 100 $\mu$M AZT this volume decrease is diminished to 119.8 ± 0.7%. Thus RVD is significantly reduced from 30.3 ± 3% to 16.6 ± 3% in the presence of AZT (insert). The swelling experiments are given as actual volumes (V) divided by $V_0$, where $V_0$ is the mean of the first five measurements prior to the reduction of extracellular osmolarity versus time. RVD is expressed as loss of cell volume within 240 sec relative to the volume gained by the cells 60 sec after imposing the osmotic gradient. (d) The sensitivity of AZT for the cAMP-activated chloride current ($I_{ClcAMP}$) was measured in CaCo cells. In the presence of dbcAMP (0.5 mM), forskolin (0.01 mM), and IBMX (0.1 mM) a chloride current can be elicited ranging from +102.4 ± 60.3 pA ($n = 5$) to + 602.6 ± 189.9 pA ($n = 5$). Extracellular AZT in a concentration of 100 $\mu$M is without any significant effect on $I_{ClcAMP}$ (+508.8 ± 191.1 pA; $n = 5$). NPPB in a concentration of 0.5 mM significantly reduces $I_{ClcAMP}$ to +120.0 ± 28.9 pA ($n = 5$).

channels leads to an impaired ability of cells to regulate their volume back to "normal" after swelling [regulatory volume decrease (RVD) (8,12)]. Accordingly, as shown in Fig. 4c the addition of 100 $\mu$M AZT to H9 cells dramatically reduces RVD from 30.3 $\pm$ 2.6% ($n$ = 6) to 16.6 $\pm$ 2.3% ($n$ = 9).

## AZT Does Not Block the cAMP-Dependent Chloride Current in CaCo Cells

Blockers known to impede chloride channels poorly discriminate between the different chloride channel families (8). For better understanding of the effect of AZT on different cell systems it is essential to know if other chloride channels beside the swelling-dependent one can be blocked by this drug. To test whether cAMP-dependent chloride current is sensitive to AZT applied to the extracellular solution, we activated this current in colon carcinoma (CaCo) cells by adding a mixture of dibutyryl-cAMP (0.5 mM), forskolin (0.01 mM), and IBMX (0.1 mM) to the extracellular solution. The experiments are summarized in Fig. 4d. Two to three minutes after the addition of the mixture, a cAMP-stimulated chloride current is elicited in these cells. The cAMP-dependent chloride current cannot be changed significantly by the addition of 100 $\mu$M AZT. Replacing AZT with 0.5 mM NPPB, a known blocker of chloride currents (14), however, dramatically reduces the current to similar values to those prior to stimulation (Fig. 4d).

## Volume Measurements in Fibroblasts Treated with AZT and/or HSV

As discussed above, AZT substantially reduces RVD in H9 cells. $I_{Cl}$ is crucial for controlling the cell volume and reducing the cytoplasmatic volume after swelling. Since the resting volume of cells is lower than the equilibrium (15), blocking $I_{Cl}$ in resting cells should increase their volume. Also, this swelling effect of substances able to block $I_{Cl}$ could be intensified in virus-infected cells, which are known to show cytoplasmatic swelling after infection with a variety of different viruses (16–23). To test for this effect of AZT in either uninfected fibroblasts or fibroblasts infected with herpes simplex virus (HSV), cell volumes were determined under the different experimental conditions. The absolute cell volume of fibroblasts was measured 12, 24, and 34 hr after reculture (see Materials and Methods). In untreated cells (control in Fig. 5), the cytoplas-
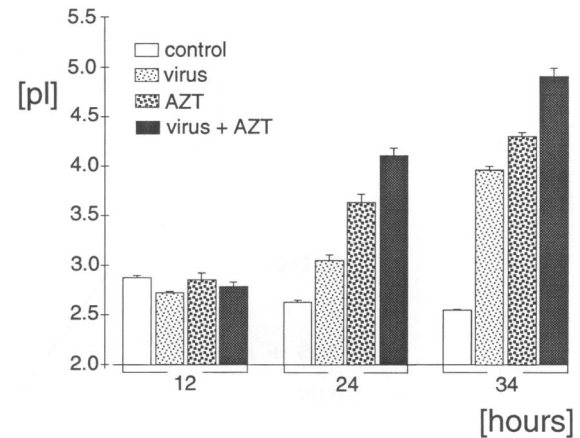


**FIG. 5. Cell volume measurements in NIH 3T3 fibroblasts in the presence and absence of AZT and in fibroblasts infected with HSV in the presence and absence of AZT**

The absolute cell volumes (in pl) were measured 12, 24, and 34 hr after reculturing the cells. Conditions were changed immediately before the time point of 12 hr. At this point cells were exposed to AZT, virus (HSV at an m.o.i. of >10) or both. For controls the cell volumes of untreated cells were measured at the equivalent time points.

matic volume of single cells diminished from 2874 $\pm$ 25 fl ($n$ = 3) to 2628 $\pm$ 19 fl ($n$ = 4) and 2548 $\pm$ 10 fl ($n$ = 4) at the time points measured. Twelve hours after reculturing the cells, AZT, AZT and HSV, or HSV alone, were added to the cells and their volume determined immediately, then 12, and 22 hr after incubation. Fibroblasts infected with HSV (HSV strain *wal*, [24]) at a multiplicity of infection (m.o.i.) of >10 (Fig. 5) increase their volume from 2725 $\pm$ 8 fl immediately after adding the virus, to 3050 $\pm$ 56 fl and 3955 $\pm$ 46 fl (SEM; $n$ = 4). HSV strain *wal* was chosen for its ability to infect fibroblasts with high efficiency (>95%), which is mandatory for the volume measurements. The addition of AZT alone increases the cell volume even further than virus infection alone. Twelve and twenty-two hours after adding the drug, the volume of the cells was 3631 $\pm$ 84 and 4301 $\pm$ 38 fl ($n$ = 4). Infection of the cells in the presence of AZT leads to a significantly larger increase in volume (4107 $\pm$ 73 and 4912 $\pm$ 83 fl, $n$ = 4; Fig. 5).

## Viability Measurements of Virus-Infected Fibroblasts

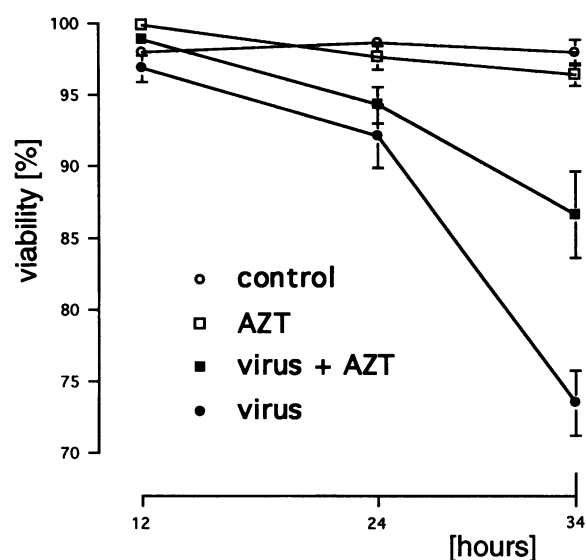The dramatic increase of the volume of virus-infected cells in the presence of AZT might sug-

**FIG. 6. Viability measurements of NIH 3T3 fibroblasts under control conditions (open symbols) and NIH 3T3 fibroblasts infected by HSV (filled symbols) in the absence and presence of AZT**

Cell viability 12, 24, and 34 hr after splitting is expressed as percentage of total cell number in a given area.

gest a reduced viability of these cells, leading to impaired virus replication. To test for this hypothesis, the viability of fibroblasts was measured at the same time points used for volume measurements. As shown in Fig. 6, cell viability in the presence of 100 $\mu$M AZT is indistinguishable from that measured in the untreated cell population. The infection of fibroblasts with the HSV strain *wal* at a m.o.i. of >10 dramatically reduces the viability from 96.4 $\pm$ 1% to 73.5 $\pm$ 2% after 22 hr of virus infection. After the same period of infection, viability is significantly higher (86.7 $\pm$ 3%) in the presence of AZT. The results indicate that the increased cytoplasmatic volume of virus-infected cells in the presence of AZT is not accompanied by reduced viability of the infected cells within the time measured. We cannot rule out, however, that the increased cytoplasmatic volume in virus-infected cells negatively affects virus replication.

## DISCUSSION

Decreasing extracellular osmolarity leads to the activation of an outwardly rectifying chloride current, $I_{Cl}$, in NIH 3T3 fibroblasts. In H9 cells, a similar current can be elicited with properties identical to those of $I_{Cl}$ in fibroblasts. Antisense oligonucleotides complementary to $I_{Cln}$, a cloned chloride channel from MDCK cells (1) reduces $I_{Cl}$ in these fibroblasts (5), indicating that $I_{Cln}$ is the chloride channel itself or a closely related protein (25). The simplest explanation at present is that $I_{Cln}$ is the chloride channel itself, as previously described (5,8). However, a more complex interaction between $I_{Cln}$ and pre-existing proteins cannot be ruled out. A unique feature of the swelling-induced chloride current is its sensitivity to different nucleotides. $I_{Cln}$ expressed in *Xenopus* oocytes can be blocked by the extracellular addition of cGMP, ITP, cAMP, GTP, ATP, ADP, or AMP (1). $I_{Cl}$ activated in fibroblasts can be blocked by cAMP, ATP, or cGMP (5). The molecular structures of AZT or acyclovir used in therapy of viral infections are closely related to the nucleotides tested. As we show here, both AZT and acyclovir are able to dramatically and instantaneously impede $I_{Cl}$ in fibroblasts and H9 cells, indicating that the observed inhibition of $I_{Cl}$ reflects a direct effect on the channels. This effect is most likely not related to premature chain termination and the consecutive indirect inhibition of $I_{Cl}$. The inhibition of $I_{Cl}$ is observed at concentrations typically present in the plasma of patients treated with these drugs (26) (Figs. 1, 2, and 4). Accordingly, fluorescence optical measurements show a significant inhibition of the KSCN quench of the MEQ fluorescence expressing chloride movement across the cell membrane (Fig. 1d). AZT is able to discriminate between the swelling-dependent chloride current $I_{Cl}$ and the chloride current activated by cAMP (Fig. 4d) leading to a selective blockage of $I_{Cl}$. Moreover, we show that AZT increases the cell volume of fibroblasts (Fig. 5). These findings support our hypothesis that $I_{Cln}$ is the swelling-induced chloride current and that AZT and acyclovir specifically block this current.

Ganciclovir, however, does not have any significant effect on $I_{Cl}$ at concentrations up to 0.1 mM. This drug, used in patients infected with cytomegalovirus, differs from acyclovir only by the addition of a hydroxymethyl group at the sugar rudiment of the acyclovir molecule (Fig. 2 a and b).

TDP, structurally related to AZT, is also unable to block $I_{Cl}$ at concentrations of up to 0.1 mM (Fig. 3a). It is, however, important that TDP is able to competitively inhibit the blocking effect of AZT on $I_{Cl}$. As shown in Fig. 3b, the addition of 100 $\mu$M TDP does not impair the swelling-

induced chloride current. In the presence of TDP, addition of AZT to the extracellular fluid has virtually no effect. However, after washing out both substances and adding 100 $\mu$M AZT, $I_{Cl}$ is substantially reduced (Fig. 3b). Similar results can be obtained for uridine and acyclovir in NIH 3T3 fibroblasts. It has been shown that the nucleoside uridine is able to reduce the cytotoxic effect of AZT in human bone marrow progenitor cells (27), as well as the neurotoxic effect of the nucleotide ddC (2',3'-dideoxycytidine) (28). Our results could provide a molecular mechanism explaining these therapeutically very important findings. In general, growing cells, neurons (and/or their surrounding glial cells), and cells with a large substrate transport and therefore high volume stress (e.g., epithelial cells in the gastrointestinal tract or tubular cells in the kidney) need powerful mechanisms to regulate their cytoplasmatic volume (15). Impairing the swelling-induced chloride current leads to a reduced regulatory volume decrease, cell swelling and, as a result, impaired organ function (15). The cytotoxic effects observed in patients treated with antiviral drugs from the nucleoside analog family are mainly restrained to bone marrow, gastrointestinal, kidney, and neuronal functions. The side effects of these drugs could be due to a block of the swelling-induced chloride current. It can be speculated that the simultaneous administration of TDP or uridine, as nonactive molecules able to bind to the chloride channel, together with AZT or acyclovir, could reduce the side effects provoked by these antiviral drugs. Additional substances, which could substitute for TDP or uridine in protecting $I_{Cl}$ more efficiently, are currently under investigation. Moreover, a substantial increase of the dosage of antiviral drugs of the nucleoside analog family could be feasible in conjunction with such competitive inhibitors. The role of cell swelling in virus replication is, however, still unclear. The viability of virus-infected cells, additionally swollen in the presence of AZT (Fig. 5), is not reduced when compared with that of cells infected with virus alone (Fig. 6). A direct influence of blocking RVD on virus replication by reducing viability of infected cells can be ruled out. It remains, however, to be tested if and how swelling itself affects virus replication. Such an effect could be mediated by a change in the "internal milieu" observed after cell swelling. Intracellular ions like potassium and chloride, and the intracellular pH, are reduced under this condition (29,30). In addition, the intracellular bioactive calcium concentration (Ref. 31 and our own unpublished results) is increased in swollen cells, changing different biochemical pathways (32,33). Additional experiments need to be done to determine if cell swelling could lead to a modulation of the specific sensitivity of different viruses for certain antiviral drugs.

In conclusion, our experiments show a novel molecular mechanism by which antiviral drugs of the nucleoside analog family could lead to impairments of the kidney, bone marrow, gastrointestinal, and neuronal functions, and how these side effects could possibly be restricted by the presence of TDP or uridine as competitive inhibitors for $I_{Cl}$ blockage.

## ACKNOWLEDGMENTS

## REFERENCES

1. Paulmichl M, Li Y, Wickman K, Ackerman M, Peralta E, Clapham D. (1992) New mammalian chloride channel identified by expression cloning. *Nature* **356:** 238–241.
2. Alton EWFW, Manning SD, Schlatter PJ, Geddes DM, Williams AJ. (1991) Characterization of a $Ca^{2+}$-dependent anion channel from sheep tracheal epithelium incorporated into planar bilayers. *J. Physiol.* **443:** 137–159.
3. Vanglarik CJ, Singh AK, Wang R, Bridges RJ. (1993) Trinitrophenyl-ATP blocks colonic $Cl^-$ channels in planar phospholipid bilayers. Evidence for two nucleotide binding sites. *J. Gen. Physiol.* **101:** 545–569.
4. Zhang J, Smith T, Lobaugh L, Hall S, Lieberman M. (1992) Cyclic AMP inhibits the swelling activated ICl associated with cardiac cell volume regulation. *Physiologist* **35:** 18. Abstract.
5. Gschwentner M, Nagl UO, Wöll E, Schmarda A, Ritter M, Paulmichl M. (in press) Anti-

sense oligonucleotides suppress cell volume-induced activation of chloride channels. *Pflügers Arch.*

6. Marty A, Neher E. (1983) Tight-seal whole-cell recording. In: Sakmann B, Neher E (eds). *Single-Channel Recording*. Plenum Press, New York, pp. 107–122.

7. Bubien JK, Kirk KL, Rado A, Frizzell RA. (1990) Cell cycle dependence of chloride permeability in normal and cystic fibrosis lymphocytes. *Science* **248:** 1416–1419.

8. Paulmichl M, Gschwentner M, Wöll E, et al. (1993) Insight into the structure-function relation of chloride channels. *Cell Physiol. Biochem.* **3:** 374–387.

9. Paulmichl M, Lang F. (1988) Enhancement of intracellular calcium concentration by extracellular ATP and UTP in Madin Darby canine kidney cells. *Biochem. Biophys. Res. Commun.* **156:** 1139–1143.

10. Biwersi J, Verkman AS. (1991) Cell-permeable fluorescent indicator for cytosolic chloride. *J. Biochem.* **30:** 7879–7883.

11. Kroesen BJ, Mesander G, ter Haar JG, The TH, de Leij L. (1992) Direct visualization and quantification of cellular cytotoxicity using two colour fluorescence. *J. Immunol. Methods* **156:** 47–54.

12. Paulmichl M, Friedrich F, Maly K, Lang F. (1989) The effect of hypoosmolarity on the electrical properties of Madin Darby canine kidney cells. *Pflügers Arch.* **413:** 456–462.

13. Ritter M, Steidl M, Lang F. (1991) Inhibition of ion conductances by osmotic shrinkage of Madin-Darby canine kidney cells. *Am. J. Physiol.* **261:** C602–C607.

14. Wangemann P, Wittner M, Di Stefano A, et al. (1986) Cl⁻-channel blockers in the thick ascending limb of the loop of Henle. Structure activity relationship. *Pflügers Arch.* **407:** S128–S141.

15. Lang F, Ritter M, Völkl H, Häussinger D. (1993) The biological significance of cell volume. *Renal Physiol. Biochem.* **16:** 48–65.

16. Abdul-Aziz TA, Arp LH. (1983) Progression of tracheal lesions in turkeys exposed by aerosol to LaSota strain of Newcastle disease virus. *Avian Dis.* **27:** 1131–1141.

17. Bardadin KA, Scheuer PJ. (1984) Endothelial cell changes in acute hepatitis. A light and electron microscopic study. *J. Pathol.* **144:** 213–220.

18. Bashford CL, Micklem KJ, Pasternak CA. (1985) Sequential onset of permeability changes in mouse ascites cells induced by

19. Karayiannis P, Petrovic LM, Fry M, et al. (1989) Studies of GB hepatitis agent in tamarins. *Hepatology* **9:** 186–192.

20. McNutt NS, Kindel S, Lugo J. (1992) Cutaneous manifestations in measles in AIDS. *J. Cutaneous Pathol.* **19:** 315–324.

21. Nagra RM, Burrola PG, Wiley CA. (1992) Development of spongiform encephalopathy in retroviral infected mice. *Lab. Invest.* **66:** 292–302.

22. Neser JA, Phillips T, Thomson GR, Gainaru MD, Coetzee T. (1986) African swine fever. I. Morphological changes and virus replication in blood platelets of pigs infected with virulent haemadsorbing and non-haemadsorbing isolates. *Onderstepoort J. Vet. Res.* **53:** 133–141.

23. Pohlenz JF, Cheville NF, Woode GN, Mokresh AH. (1984) Cellular lesions in intestinal mucosa of gnotobiotic calves experimentally infected with a new unclassified bovine virus (Breda virus). *Vet. Pathol.* **21:** 407–417.

24. Schröder C, Engler H, Kirchner HJ. (1981) Protection of mice by an apathogenic strain of HSV-1 against lethal infection by a pathogenic strain of HSV type 1. *J. Gen. Virol.* **52:** 159–161.

25. Krapivinsky GB, Ackerman MJ, Gordon EA, Krapivinsky LD, Clapham DE. (1994) Molecular characterization of a swelling-induced chloride conductance regulatory protein, $p_{Cln}$. *Cell* **76:** 439–448.

26. Jacobson MA. (1993) Valaciclovir (BW256U87): The L-valyl ester of acyclovir. *J. Med. Virol.* **1:** 150–153.

27. Sommadossi JP, Carlisle R, Schinazi RF, Zhou Z. (1988) Uridine reverses the toxicity of 3'-azido-3'-deoxythymidine in normal human granulocyte-macrophage progenitor cells in vitro without impairment of antiretroviral activity. *Antimicrob. Agents Chemother.* **32:** 997–1001.

28. Keilbaugh SA, Hobbs GA, Simpson MV. (1993) Anti-human immunodeficiency virus type 1 therapy and peripheral neuropathy: Prevention of 2',3'-dideoxycytidine toxicity in PC12 cells, a neuronal model, by uridine and pyruvate. *Mol. Pharmacol.* **44:** 702–706.

29. Lang F, Völkl H, Häussinger D. (1990) General principles in cell volume regulation. *Comp. Physiol.* **4:** 1–25.

30. Ritter M, Paulmichl M, Lang F. (1991) Fur-

ther characterization of volume regulatory decrease in cultured renal epitheloid (MDCK) cells. *Pflügers Arch.* **418:** 35–39.

31. Pierce SK, Politis AD. (1990) $Ca^{2+}$-activated cell volume recovery mechanisms. *Annu. Rev. Physiol.* **52:** 27–42.

32. Häussinger D, Lang F. (1991) The mutual interaction between cell volume and cell function: A new principle of metabolic regulation. *Biochem. Cell Biol.* **69:** 1–4.

33. Häussinger D, Lang F. (1991) Cell volume—A 'second messenger' in the regulation of metabolism by amino acids and hormones. *Cell Physiol. Biochem.* **1:** 121–130.